Characteristic transport properties of CoO-coated monodispersive Co cluster assemblies

D. L. Peng, K. Sumiyama, T. J. Konno, T. Hihara, and S. Yamamuro
Institute for Materials Research, Tohoku University, 2-1-1 Katahira, Aoba-ku, Sendai 980-8577, Japan
and CREST of Japan Science and Technology Corporation, Kawaguchi 332-0012, Japan
(Received 19 January 1999)

We have fabricated CoO-coated monodispersive Co cluster assemblies with the mean cluster size of 13 nm at various oxygen gas-flow rate R_{O_2} by a plasma-gas-condensation-type cluster beam deposition technique, and studied their electrical conductivity, σ, and magnetoresistance. For $R_{O_2}<0.24$ SCCM (sccm denotes cubic centimeter per minute), the resistivity revealed a minimum and showed $\ln T$ dependence at lower temperatures, probably due to the weak localization of conduction electrons owing to presence of thin oxide shells covering Co cores. A small negative magnetoresistance was observed in this regime. For $R_{O_2}>0.3$ SCCM, tunnel-type temperature dependence of σ in the form of $\ln \sigma$ vs $1/T$ was observed between 7 and 80 K. This differs from the well-known temperature dependence of $\ln \sigma$ vs $1/T^{1/2}$ for disordered granular materials. The magnetoresistance ratio, $(\rho_{H=30\,kOe}-\rho_0)/\rho_0$, is negative and its absolute value increases sharply with decreasing temperature below 25 K: from 3.5% at 25 K to 20.5% at 4.2 K. This marked increase, by a factor of 6, is much larger than those observed for conventional metal-insulator granular systems. These results are ascribed to a prominent cotunneling effect in the Coulomb blockade regime, arising from the uniform Co core size and CoO shell thickness in the present monodispersed cluster assemblies. [S0163-1829(99)06527-3]

I. INTRODUCTION

Meiklejohn and Bean[1] first discovered the exchange anisotropy effect, which originates from a strong exchange coupling between the ferromagnetic Co core and the antiferromagnetic CoO layer in oxide-coated Co particles prepared by electrodeposition onto a mercury cathode. Much attention has been focused on the magnetic properties and the unidirectional exchange anisotropy in oxide-passivated magnetic transition-metal particles including Fe,[2] Co,[3–5] and Ni (Refs. 6,7) because of their potential application. However, no study on the electrical transport properties and magnetoresistance of the oxide-coated Co particles has been reported so far. Recently, we have reported the electrical conductivity and magnetoresistance of a CoO-coated monodispersive Co cluster assembly fabricated by a plasma-gas-condensation (PGC)-type cluster beam deposition technique.[8] The enhancement of the magnetoresistance ratio at low temperature was much larger than those observed for conventional metal-insulator granular systems.

Giant magnetoresistance (GMR) has been observed in a structure of two ferromagnetic layers separated by a thin insulator (FM/I/FM).[9] Such GMR arises from a spin-dependent tunneling effect. Electron tunneling between two ferromagnetic electrodes through an insulating layer depends on the relative orientation of the magnetizations of the electrodes. When the relative orientation of the magnetizations is changed by applying a magnetic field, tunnel-type magnetoresistance (TMR) is expected to occur. Although this effect was discovered by Julliere[10] in 1975, and subsequently in several other FM/I/FM junctions,[11,12] large and reproducible TMR ratios have been found only recently.[13,14]

In FM-I granular systems, where the magnetic metal granules or clusters are embedded in an insulating matrix, the TMR effect has also been detected,[15] including a large TMR reported recently.[16] For these materials, when the metal cluster concentration is just below the percolation threshold, the electrical conduction is dominated by the tunneling between metallic clusters, with the tunnel resistance enhanced by the Coulomb blockade at low temperatures. The tunnel current between randomly oriented magnetic granules is smaller than that between the magnetically aligned ones. Since conventional granular materials have been produced by codeposition of a metal and an oxide, and subsequent precipitation of magnetic granules on a substrate, there is normally a wide distribution of the cluster size and intercluster distance (namely the tunnel-barrier thickness). In such heterogeneous granular systems, the low-field conductivity is known to follow the $\exp(-b/T^{1/2})$ law for a wide temperature range.[17]

The present work explores in detail the structural, and electrical and magnetic transport properties of the CoO-coated monodispersive Co cluster assemblies. First, we elucidate their morphology by transmission electron microscopy (TEM). We then measured the temperature dependence of the electrical conductivity and TMR in these cluster assemblies. In particular, we emphasize that the monodispersed Co cluster size distribution and a nearly uniform thickness of the CoO shells give rise to the distinct features in their electrical conductivity and TMR. It should be noted that cobalt (II) oxide CoO is an antiferromagnetic semiconductor with the Néel temperature of 293 K. The room-temperature resistivities of CoO single crystals are $10^8-10^{15}\,\Omega$-cm, and the activation energies are 0.73–1.35 eV.[18]

II. EXPERIMENT

Our samples were fabricated with a PGC-type cluster beam deposition apparatus, which is a combination of sputtering and gas-condensation techniques.[8,19] The PGC-type cluster beam deposition apparatus is mainly composed of three parts: a sputtering chamber, a cluster growth room and a deposition chamber. The vaporized atoms in the sputtering

chamber are decelerated by the collisions with a large amount of Ar gas injected continuously into the sputtering chamber [the Ar gas flow rate: $R_{Ar}=250-500$ SCCM (sccm denotes cubic centimeter per minute], and are swept into the cluster growth room, whose inner wall is cooled by liquid nitrogen. The clusters formed in this room are ejected from a small nozzle by differential pumping and a central part of the cluster beam is intercepted by a skimmer, and then deposited onto a sample holder in the deposition chamber ($10^{-5}-10^{-4}$ Torr). Using this system, we obtained mono dispersed transition metal clusters having the mean size of 6-14 nm and the standard deviation less than 10% of the mean size.[19] In this study, we examine the electrical transport properties and TMR of the CoO-coated monodispersive Co cluster assemblies with the mean cluster diameter of $d=13$ nm. We introduced oxygen gas through a nozzle near the skimmer into the deposition chamber to form CoO shells on the Co clusters before depositing onto the substrate. This process ensures that all Co clusters are uniformly oxidized before the cluster assemblies are formed. For a constant R_{Ar}, the gas pressure in the deposition chamber can be adjusted to be lower than 3×10^{-4} Torr by changing the flow rate of oxygen gas R_{O_2}. Cluster assemblies with the effective thickness of about 100 nm, as measured by a quartz thickness monitor, were formed at room temperature on polyimide films and glass substrates with two precoated Au electrodes. Using the conventional four-probe method, the electrical resistivity was measured at a constant voltage because the ohmic law ceased to hold at low temperatures. The MR was measured in the applied field parallel to the electrical current direction.

A superconducting quantum interference device magnetometer was used to study the magnetic properties and magnetoresistance of the cluster assemblies in the temperature range between 4 and 390 K, and in magnetic fields up to 50 kOe. Transmission electron microscopy (TEM) was used to study the cluster size, crystal structure, and morphology of the core-shell structure.

III. RESULTS

A. Structure, morphology, and exchange interaction

The initial stage of the clusters deposited on microgrids were observed by a Hitachi HF-2000 TEM, operating at 200 kV. The TEM observation showed that the cluster size was independent of the deposition time.[20] Figure 1 shows (a) bright-field TEM images and (b) corresponding cluster size distributions in the initial stage of the oxide-coated Co cluster assemblies produced at $R_{Ar}=500$ SCCM and $R_{O_2}=0$, 0.24, and 0.44 SCCM. We estimated the cluster size distributions from digitized images recorded by a slow scan charge-coupled device (CCD) camera in the object area of 350×350 nm^2 using an image-analysis software (Image-Pro PLUS: Media Cybernetics). As shown here, the clusters are almost monodispersed, with the mean diameter of about $d=13$ nm and the standard deviation (Δ) less than 10% of the mean size. Note that the cluster size is insensitive to R_{O_2}. But as we will show later in Sec. III. *B*, the exchange interaction and electric resistivity increased with increasing R_{O_2}, which indirectly indicates that the thickness (or amount) of the antiferromagnetic cobalt oxide shell increases with increasing R_{O_2}. Figures 2(a) and 2(b) are selected area electron diffraction patterns for the samples prepared at $R_{O_2}=0.24$ and 0.44 SCCM, respectively, showing the coexistence of fcc Co and CoO phases. It is noted that the intensities of the rings of the CoO phase for the sample produced at $R_{O_2}=0.44$ SCCM [Fig. 2(b)] is stronger than those at $R_{O_2}=0.24$ SCCM [Fig. 2(a)]. This indicates that the amount of the CoO phase for the sample prepared at $R_{O_2}=0.44$ SCCM is larger than that at $R_{O_2}=0.24$ SCCM. Figure 3 is a high resolution TEM picture of a cluster connected with another cluster prepared at $R_{O_2}=0.44$ SCCM. It can be seen that a dark core is surrounded by a light contrast shell. The cross fringes in the core region, as indicated by the arrows, correspond to the {200} spacings (0.177 nm) of fcc Co. On the other hand, the shell is composed of many small grains. For example, the cross fringes in the upper left grains (indicated by the arrows) are {111} and {210} spacings of the CoO phase, and shows that this particular grain has a ⟨321⟩ axis nearly parallel to the incident electron beam. Therefore, we can conclude that the clusters prepared in the current study possess a well-defined core-shell-type structure, in which the core and the shell is composed of the metallic fcc Co and insulating CoO phases, respectively.

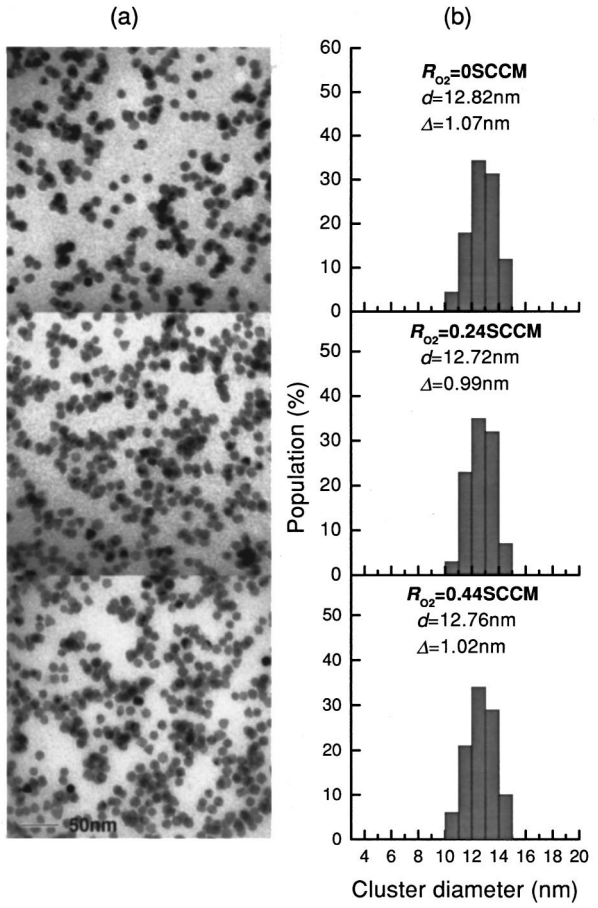

FIG. 1. (a) Bright-field TEM images and (b) cluster size distributions of the initial stage of oxide-coated monodispersed Co cluster assemblies produced at the Ar gas flow rate R_{Ar} of 500 SCCM and the O_2 gas flow rates R_{O_2} of 0, 0.24, and 0.44 SCCM.

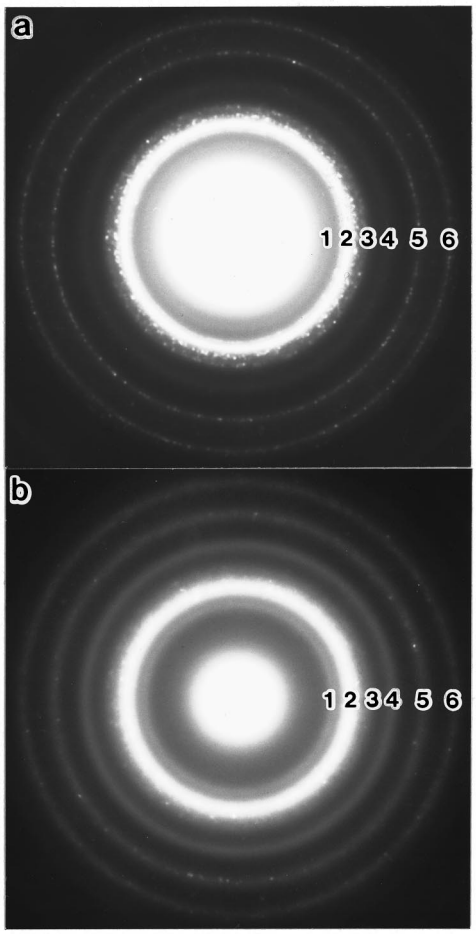

FIG. 2. Electron diffraction patterns of the oxide-coated Co cluster assemblies prepared on a carbon microgrid at (a) $R_{O_2}=0.24$ and (b) 0.44 SCCM. The diffraction rings 2, 3, 5, and 6 correspond to {111}, {200}, {220}, and {311} of the fcc-Co phase, respectively, and those 1 and 4 to {111} and {220} of the CoO phase, respectively.

In order to examine the exchange coupling arising from the presence of the CoO phase, we measured hysteresis loops and low-field thermomagnetic curves of the CoO coated Co cluster assemblies prepared at same $R_{O_2}=1$ SCCM for both zero-field cooled (ZFC) and field-cooled (FC) samples, as shown in Figs. 4 and 5. The hysteresis loops were measured at 5 K after ZFC and FC from 300 to 5 K in a magnetic field H of 50 kOe. The direction of H applied to measure the loops was parallel to that of the cooling field. The large loop shift against the direction of the cooling field is detected in the FC sample, in contrast to the symmetric feature of the ZFC sample (the shift, $\Delta H_c=H_c^{\mathrm{ZFC}}-H_c^{\mathrm{FC}}$, where H_c^{ZFC} and H_c^{FC} are indicated in Fig. 4). This confirms the presence of the unidirectional exchange anisotropy due to the strong exchange coupling between the ferromagnetic Co core and the antiferromagnetic CoO shell. Figure 5 shows the low field thermomagnetic curves, $M_{\mathrm{ZFC}}-T$ and $M_{\mathrm{FC}}-T$, for the CoO-coated Co cluster assemblies prepared at $R_{O_2}=1$ SCCM. For the ZFC or FC measurement, the sample was cooled in $H=0$ or 100 Oe, respectively, from $T=390$ to 5 K; then $H=100$ Oe was applied and the magnetization was measured with increasing temperature. As seen from Fig. 5, a

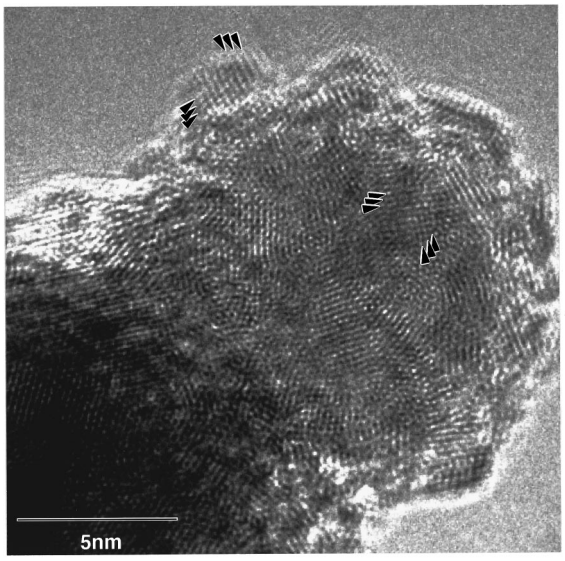

FIG. 3. A high-resolution TEM image of CoO-coated Co clusters prepared on a carbon-coated microgrid at the O_2 gas flow rate $R_{O_2}=0.44$ SCCM, showing the structure of a Co core and a surrounding CoO shell. The arrowed cross fringes inside the dark core region correspond to the {200} lattice spacing of the fcc-Co phase, while those for the upper left grains are for the {111} and {210} spacings of the CoO phase.

distinct magnetic cooling effect is observed at low temperatures. The ZFC magnetization almost remains zero below 150 K because of the strong exchange interaction between the Co core and CoO shell. This also clearly indicates that the oxide shell in our samples is composed of the single-CoO phase other than the Co_3O_4 phase, whose bulk form has a Néel temperature of about 40 K.

B. Temperature dependence of the electrical resistivity

Figure 6 shows the electrical resistivity ρ as a function of (a) temperature, T, and (b) the logarithm of temperature for the samples prepared at $R_{\mathrm{Ar}}=500$ SCCM and $R_{O_2}=0$, 0.07, 0.12, 0.24, and 0.35 SCCM. As one can see from Fig. 6, the

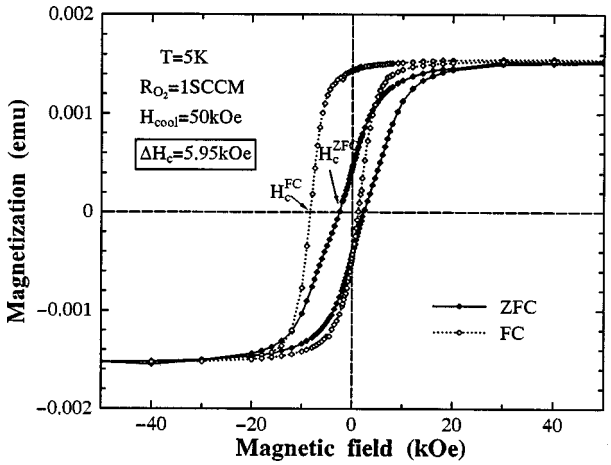

FIG. 4. Zero-field-cooled (ZFC) and field-cooled (FC) hysteresis loops of the CoO-coated Co cluster assemblies prepared at $R_{O_2}=1$ SCCM. Here, the magnetic field H_{cool} of 50 kOe was applied during the field cooling.

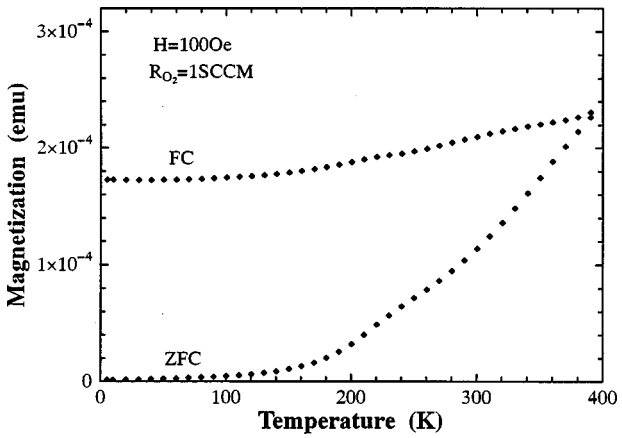

FIG. 5. Thermomagnetic curves of the ZFC and FC states of the CoO-coated Co cluster assembly prepared at $R_{O_2}=1$ SCCM. Here, the magnetic field of 100 Oe was applied during the field cooling and the measurement.

temperature dependence of ρ is clearly different for the samples prepared at different R_{O_2}. For $R_{O_2}=0$ SCCM, the sample shows ordinary metallic temperature dependence, characterized by the residual resistance at low temperatures and a linear increase with increasing T. For $0<R_{O_2}<0.24$ SCCM, the resistivity exhibits a minimum at the temperature T_{min}, which shifts to higher temperatures with increasing R_{O_2}. Above T_{min}, the samples show the metallic behavior as revealed by the linear temperature dependence of ρ. Below T_{log}, the value of ρ logarithmically increases with decreasing T and the increase of $\rho(T)$ becomes more pronounced with increasing R_{O_2}. When $R_{O_2}\geqslant 0.24$ SCCM, the resistivity minimum disappears and the temperature coefficient of resistivity (TCR) is negative below room temperature. However, it should be noted that there are obvious differences in the temperature dependence of ρ between the samples prepared at $R_{O_2}=0.24$ and 0.35 SCCM. For $R_{O_2}=0.24$ SCCM, $\rho(T)$ increases gradually with decreasing T and still shows a logarithmic increase for $T<T_{log}$, whereas, for $R_{O_2}=0.35$ SCCM, it increases dramatically with decreasing T below $T=10$ K and no longer exhibits the logarithmic temperature dependence. These results also indicate that the transport mechanism is different between the samples prepared at $R_{O_2}=0.24$ and 0.35 SCCM. As we will show in the next section, the large magnetoresistance effect also appeared at $R_{O_2}>0.3$ SCCM. Therefore, we further examined the temperature dependence of $\rho(T)$ for $R_{O_2}>0.3$ SCCM.

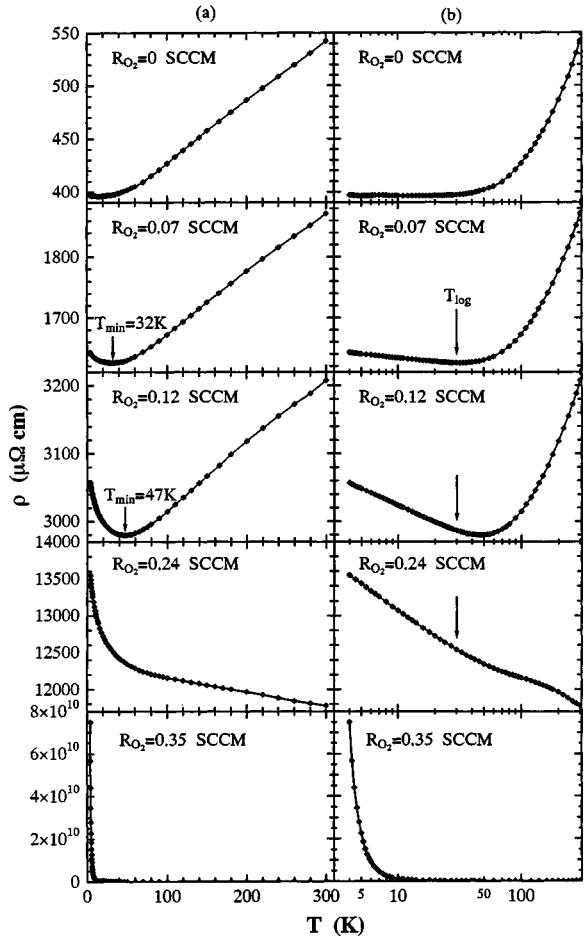

FIG. 6. (a) Electrical resistivity $\rho(T)$ at zero-magnetic field as a function of temperature T. (b) $\rho(T)$ versus logarithmic temperature for the CoO-coated Co cluster assemblies prepared at $R_{O_2}=0$, 0.07, 0.12, 0.24, and 0.35 SCCM.

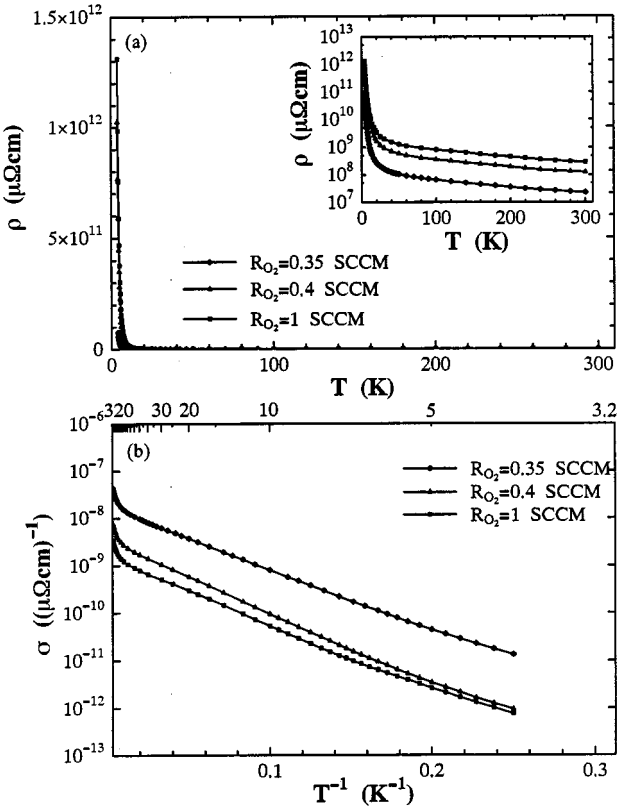

FIG. 7. (a) Temperature dependence of the electrical resistivity ρ at zero-magnetic field for the CoO-coated Co cluster assembly prepared at $R_{O_2}=0.35$, 0.4, and 1 SCCM and $\log\rho$ versus T in the inset. (b) The logarithmic conductivity $\log\sigma$ as a function of T^{-1}.

Figures 7(a) and (b) show ρ vs T and $\log\sigma$ vs $1/T$ curves, respectively, for the samples prepared at $R_{Ar}=500$ SCCM and $R_{O_2}=0.35$, 0.4, and 1 SCCM. As seen from the inset of Fig. 7(a), the resistivity at 4.2 K is three to four orders of magnitude larger than that at room temperature and about

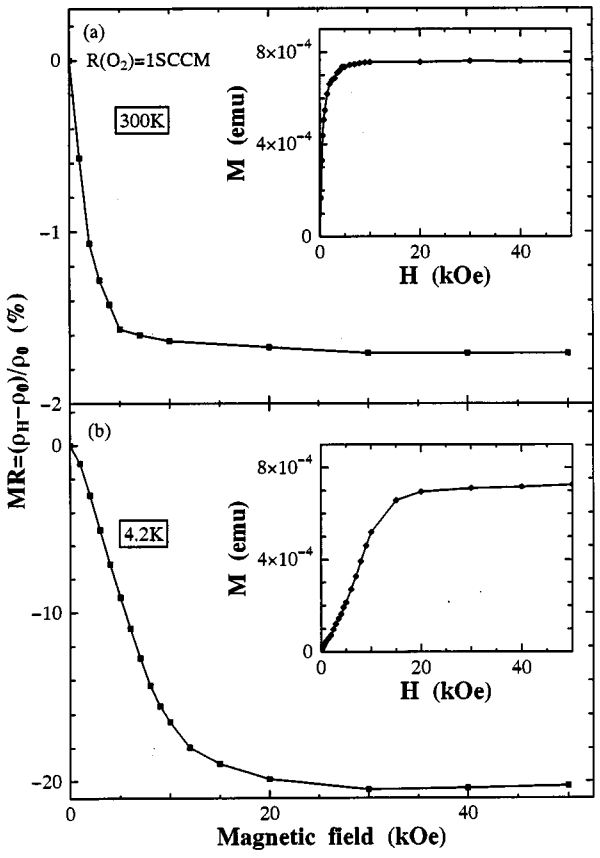

FIG. 8. Magnetic-field dependence of the magnetoresistance ratio, $MR=(\rho_H-\rho_0)/\rho_0$, at 300 and 4.2 K for the CoO-coated Co cluster assembly prepared at $R_{O_2}=1$ SCCM.

6–8 orders of magnitude larger than that of the sample prepared at $R_{O_2}=0.24$ SCCM. In addition, we find a linear dependence of $\log\sigma$ on $1/T$ in the range of $7<T<80$ K for the present CoO-coated Co cluster assemblies [Fig. 7(b)].

C. Magnetoresistance effect

Figure 8 shows the magnetoresistance ratio, $MR=(\rho_H-\rho_0)/\rho_0$, measured at 300 and 4.2 K for the CoO-coated Co cluster assembly prepared at $R_{O_2}=1$ SCCM as a function of magnetic field H applied parallel to the current direction, where ρ_0 is the resistivity of the virgin sample in the zero field. The absolute value of *MR* at 4.2 K is much larger but saturates more slowly than that at 300 K: the former saturates only above $H=30$ kOe, while the latter does so at about $H=10$ kOe. This result is well correlated with the magnetization curves shown in the insets of Fig. 8. Namely, because of the exchange interaction between the antiferromagnetic CoO shell and the ferromagnetic Co core, the magnetization curve of the CoO-coated Co cluster assembly hardly saturates at low temperatures (the Néel temperature of bulk CoO is about 291 K).

Figure 9 shows the temperature dependence of *MR* for the CoO-coated Co cluster assembly prepared at $R_{Ar}=500$ SCCM and $R_{O_2}=1$ SCCM. As seen in Fig. 9, the absolute value of *MR* increases only slightly with decreasing temperature in the range of $25<T<300$ K, while it increases rapidly below 25 K: from 3.5% at 25 K to 20.5% at 4.2 K.

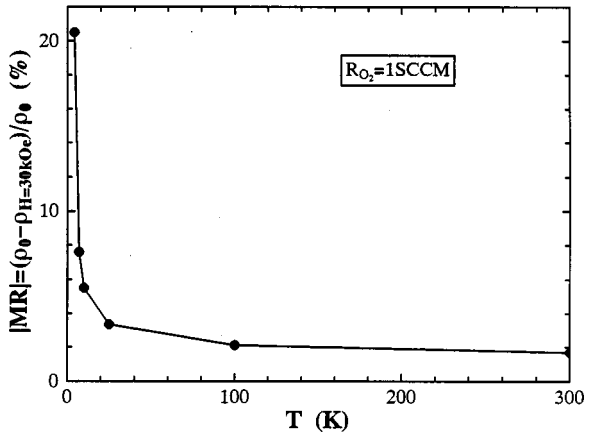

FIG. 9. Temperature dependence of the absolute value of the magnetoresistance ratio $|MR|$ at $H=30$ kOe for the CoO-coated Co cluster assembly prepared at $R_{O_2}=1$ SCCM.

Figure 10 shows the bias voltage (V_B) dependence of the resistivity (ρ) and $|MR|$ measured at 4.2 K for the CoO-coated Co cluster assembly prepared at $R_{O_2}=0.44$ SCCM. As one can see here, the resistivity decreases more than one order of magnitude with increasing V_B below 10 V. On the other hand, the absolute value of *MR* decreases by only a factor of two with increasing V_B below 40 V and is found to be insensitive to V_B above 40 V. The observed decrease of $|MR|$ with V_B is not so pronounced as that reported for ferromagnetic tunnel junctions.[13,14]

IV. DISCUSSION

Figure 11 summarizes the zero-field resistivity and *MR* at 30 kOe, measured at 4.2 and 300 K, of the CoO-coated Co cluster assemblies as a function of R_{O_2}. As shown here, the residual resistivity is about 400 $\mu\Omega\cdot$cm for the sample prepared at $R_{O_2}=0$ SCCM. This high value is ascribed to the low-density packing and weak electrical contact of the deposited clusters. Introducing the oxygen gas into the deposition chamber to form the oxide layer on the Co cluster causes the appearance of the minimum in the resistivity curve for $R_{O_2}<0.24$ SCCM. It was found that the resistivity at tem-

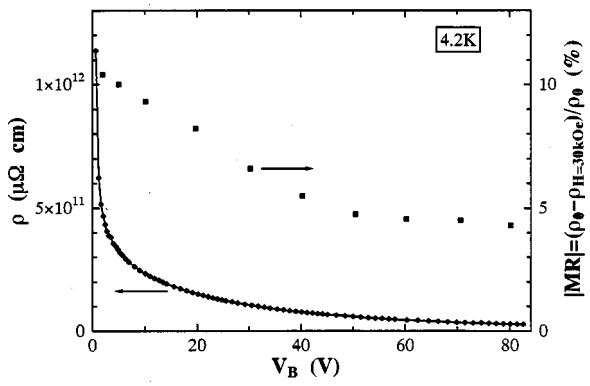

FIG. 10. Resistivity ρ and the absolute value of the magnetoresistance ratio $|MR|$ as a function of the bias voltage V_B measured at 4.2 K for the CoO-coated Co cluster assembly prepared at $R_{O_2}=0.44$ SCCM.

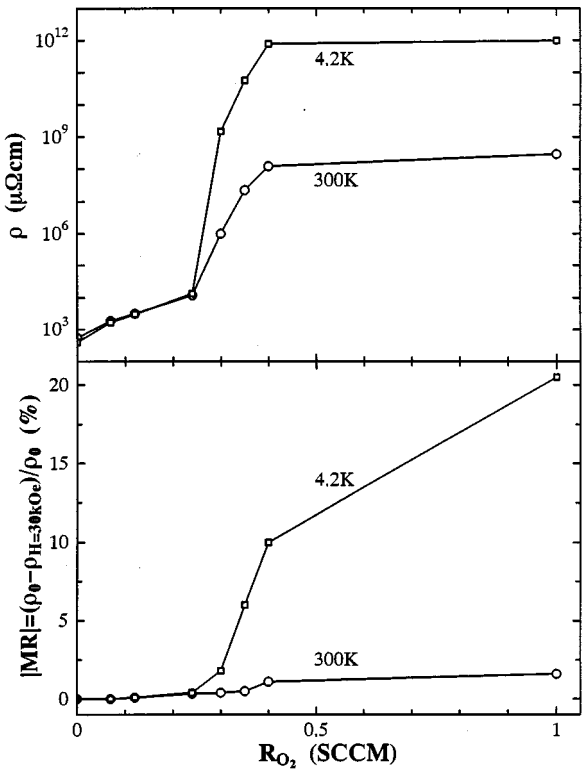

FIG. 11. Variation of (a) resistivity ρ and (b) the absolute value of the magnetoresistance ratio $|MR|$ at 300 and 4.2 K for the CoO-coated Co cluster assemblies as a function of the O_2 gas flow rate R_{O_2}.

peratures lower than $T_{\log}$ exhibits logarithmic temperature dependence (see Fig. 6).

Figures 12(a), 12(b), and 12(c) show I-V characteristics of the samples prepared at $R_{O_2}=0.12$, 0.24, and 0.35 SCCM, respectively. When $R_{O_2}=0.12$ SCCM, the resistivity shows a metallic behavior as revealed by the linear I-V characteristics [Fig. 12(a)]. Although the resistivity minimum disappears and the temperature coefficient of resistivity (TCR) becomes negative up to $T=300$ K for $R_{O_2}=0.24$ SCCM [Fig. 6(a)], the resistivity still shows a logarithmic behavior at $T<T_{\log}$, and the I-V characteristics is linear at 300 K and slightly nonlinear at 4.2 K [Fig. 12(b)]. This suggests that the conduction mechanism is the same for the samples prepared at $0<R_{O_2}<0.24$ SCCM. Such a resistivity minimum with the logarithmic temperature dependence has been also observed in many systems, such as amorphous alloys,[21,22] Al/Ni,[23] Mo/Ni,[24] and Nb/Ni (Ref. 25) multilayers, Co-Al-O (Ref. 26) and Pd-C (Ref. 27) granular films etc. The observed conductivity behavior in these systems has been ascribed to various kinds of structural and magnetic heterogeneities,[22,26] a weak-localization effect[23–27] and an electron-electron interaction.[27] In the present CoO-coated Co cluster assemblies with the logarithmic temperature dependence of the resistivity, we have observed a small negative magnetoresistance effect ($|MR|<0.4\%$), which does not strongly depend on temperature in the lower temperature region, similar to the observation for the Co-Al-O granular system.[26] In the case of the multilayers[23–25] and Pd-C granular films,[27] on the other hand, a small positive magnetoresistance effect was observed. At

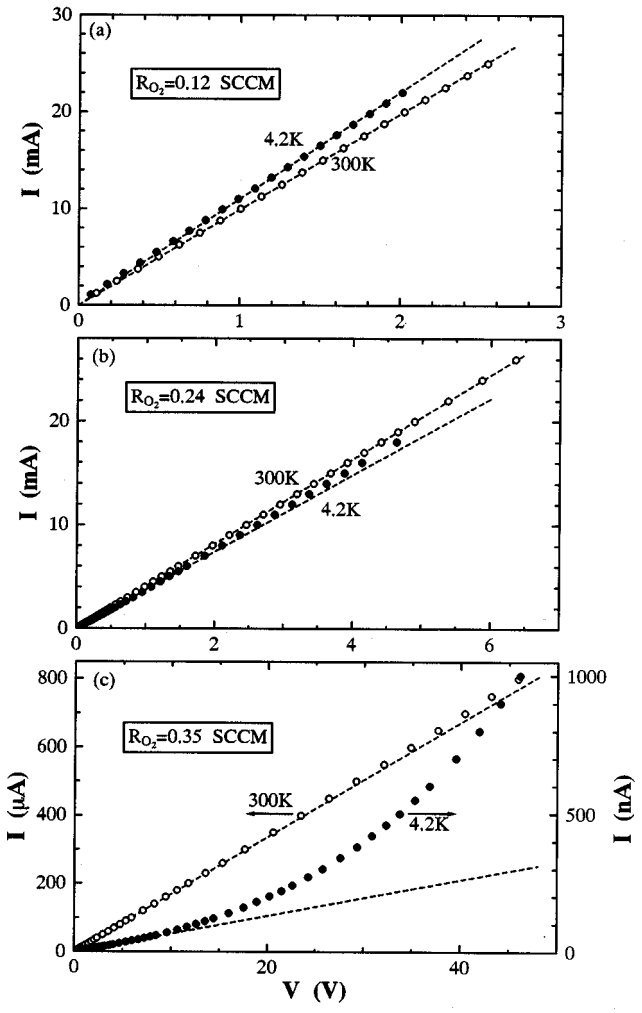

FIG. 12. Current I versus voltage V characteristics at 300 and 4.2 K for the CoO-coated Co cluster assemblies prepared at $R_{O_2}=(a)$ 0.12, (b) 0.24, and (c) 0.35 SCCM.

present, we cannot find a decisive mechanism for the logarithmic temperature dependence of the resistivity, because the $\ln T$ dependence of ρ is only predicted for a two-dimensional disordered system[28] and is not expected for manifestly three-dimensional systems in which the specimen thicknesses are more than one order of magnitude larger than the cluster size. However, we noticed that the logarithmic behavior was observed only in the samples prepared at $R_{O_2}<0.3$ SCCM, namely in the samples the real tunneltype conduction is not observed. In this region, the amount of the cobalt oxide formed is small, as can be seen in Fig. 2, because we prepared the samples under low oxygen partial pressures. The Co clusters are probably not separated completely by thin cobalt-oxide layers or the oxide interface between the Co clusters is very thin due to lack of oxygen. In such Co cluster assemblies, there are the cluster chains with quasimetallic contact (i.e., either with metallic ''point'' connections or with very thin insulating oxide barriers with negligible activation energy). In the present CoO-coated Co cluster assemblies, it is possible that the cluster chains will form a network with many cross connections between the parallel paths. Fractal dimensionality of the infinite cluster network is equal to two in a three-dimensional system at the

percolation threshold.[29,30] In this context, the logarithmic temperature dependence of the resistivity of the CoO-coated Co cluster assemblies is attributable to the weak-localization effect in the quasi-two-dimensional cluster network. At low temperatures, the resistivity that increases with lowering the temperature is dominated by quantum interference of conduction electrons.

In the conventional granular systems,[26,27] when the degree of disorder is increased, a metal-insulator transition takes place at a critical metal volume fraction x_p. A dramatic increase in the resistivity is expected to occur because the percolation of electrical contact through the metallic network is broken down in the mixed phase. As seen in Fig. 11, the resistivity at 4.2 K for $R_{O_2} > 0.3$ SCCM is about 6–8 orders of magnitude larger than that for $R_{O_2} = 0.24$ SCCM and the *MR* starts to increase rapidly with increasing R_{O_2}. Such an abrupt increase in the resistivity of the present cluster assemblies is attributable to the tunneltype conduction between metallic Co clusters via CoO shell layers. Moreover, as one can see from Fig. 12(c), the I-V characteristics for $R_{O_2} = 0.35$ SCCM slightly deviates from the ohmic linear relation at higher *V* at 300 K and clearly becomes non-linear at 4.2 K, similar to the I-V characteristics in the regime of the tunneltype conduction of the conventional metal-insulator granular systems.

The low-field tunneltype electrical conduction in granular materials was discussed by Neugebauer and Webb.[31] Most simply, the conductivity is expressed as follows:

$$\sigma \propto \exp(-2\kappa s - E_c/2k_BT), \tag{1}$$

where *s* is the tunnel-barrier thickness between the two clusters, κ the tunneling exponent of electron wave functions in the insulator, i.e., $\kappa = [2m^*(\phi + E_F - E)/\hbar^2]^{1/2}$; m^* the effective electron mass, ϕ the barrier height, *E* the electron energy, E_F the Fermi level, and $\hbar$ the Plank constant. E_c is the electrostatic energy required to create a positive-negative charged pair in two clusters by tunneling, and gives rise to the Coulomb blockade effect at a low temperature. When the applied voltage and thermal energy are much smaller than E_c, electrons or holes can not tunnel from one neutral cluster to another without exciting their states from the Fermi level to the levels higher than E_c. When the cluster size is monodispersed and the intercluster distance (namely the same barrier thickness) uniform, Eq. (1) predicts a simple hopping-type temperature dependence for the low-field conductivity: $\sigma(T) \propto \exp(-E_c/2k_BT)$.[31] As shown in Fig. 7(b), a linear behavior of $\log\sigma$ vs $1/T$ was observed in the range of $7 < T < 80$ K for the present CoO-coated Co cluster assemblies. This temperature dependence of $\sigma(T)$ is different from the form of $\log\sigma$ vs $1/T^{1/2}$, commonly observed in the metal-insulator granular systems. We can estimate E_c of the Co core clusters from the linear part of the plot of $\log\sigma$ vs $1/T$: $E_c = 5.2$, 6, and 5.8 meV for $R_{O_2} = 0.35$, 0.4, and 1 SCCM, respectively, which are in agreement with the calculated value of 5.4 meV using the expression:[32] $E_c = (e^2/2\pi\varepsilon_0\varepsilon d)[s/(d/2+s)]$, where ε is the dielectric constant (12.9 for CoO), $\varepsilon_0 = 8.854\times10^{-12}$ F/m, *d* is the mean diameter of the Co cores (11 nm) and *s* is the separation between neighboring Co cores (2 nm). The estimated charging energy corresponds to the thermal energy of k_BT with $T \approx 70$ K. This implies that when $T > 70$ K, the normal activationtype conduction is restored because the charging energy is overcome by the thermal energy. In addition, as seen from Fig. 7(b), the conductivity abruptly increases with increasing temperature above 80 K and the estimated activation energy is about 0.02 eV at $T > 150$ K. This behavior is ascribable to polaron band-hopping conduction in the nonstoichiometric CoO semiconductor shell because there are usually a large number of defects and excess carriers in the transition metal oxides.

Looking at Figs. 7(a) and 9, there is a good correlation between the magnetoresistance ratio and the resistivity at low temperatures: both the resistivity and $|MR|$ increase drastically with decreasing temperature. Such a remarkable enhancement of $|MR|$ at low temperatures was also observed in micrometer-sized ferromagnetic tunnel junctions,[33] single-electron transistors consisting of ferromagnetic metals (Ni/NiO/Co/NiO/Ni) (Ref. 34) and double ferromagnetic tunnel junctions with small ferromagnetic islands ($Co/Al_2O_3/Co$).[35] As shown in Fig. 9, $|MR|$ increases by a factor of six with decreasing temperature from 25 to 4.2 K in the present CoO-coated Co cluster assembly. This increase is much larger than the reported ones for the ferromagnetic junction with the Coulomb blockade effect[35] and the FM-I granular systems with a broad distribution of the size and intergranule distance.[36] Such a remarkable enhancement was also predicted by Takahashi and Maekawa[37] in the theoretical study on the spin-dependent tunneling with the Coulomb blockade for a double ferromagnetic junction containing a small metallic island. In their model, at high temperatures, the conductance of the sequential tunneling (ST) channel is much larger than that of the cotunneling (CT) channel, so that the current is carried by the ST channel and the magnetoresistance is low; at low temperature, the conductance of the ST channel becomes much smaller (Coulomb blockade) so that the main conduction is through the cotunneling processes (unblockade channel), and thus the magnetoresistance is high. In this case, the enhancement of the TMR is due to the onset of the unblocked cotunneling processes in the Coulomb blockade regime. Quite recently, Mitani *et al.*[36] have reported magnetotransport phenomena in the Co-Al-O insulating granular systems. According to their higher-order cotunneling model, the anomalous increase of the magnetoresistance at low temperatures is due to the successive onset of higher-order processes of spin-dependent tunneling between large granules through intervening small ones with strong Coulomb blockade. They have indicated that the size distribution plays an important role for TMR. As revealed in Figs. 1 and 3, however, the present CoO-coated Co cluster assemblies are monodispersive, having a well-defined Co core size and CoO shell thickness. Thus, a large amount of Co cores enter into the Coulomb blockade regime in a narrow temperature range, so that it yields a more prominent cotunneling effect. Therefore, the TMR enhancement in the Coulomb blockade regime is more remarkable than that in the FM-I granular systems prepared by the conventional precipitation process.

V. CONCLUSION

We have fabricated a CoO-coated monodispersive Co cluster assemblies using the PGC-type cluster beam deposi-

tion technique. When we have prepared the samples at the low-oxygen gas flow rate, the electrical resistivity reveals a minimum at low-temperature range. The resistivity linearly increases with increasing the temperature at $T > T_{\min}$, while it increases with decreasing T and follows $\ln T$ dependence at $T < T_{\min}$. The logarithmic behavior at low temperatures is attributable to the weak-localization effect in the quasi-two-dimensional network of Co clusters intervened by CoO layer. When we have prepared the samples at the high-oxygen gas flow rate, the tunneltype conduction is observed. The uniform Co core size and CoO surface layer (barrier) thickness in the present cluster assemblies give the tunneltype temperature dependence of $\log \sigma$ vs $1/T$ in the range of $7 < T < 80$ K. The tunneling conduction is spin dependent, leading to the large magnetoresistance. At low temperatures, the enhanced magnetoresistance is due to the Coulomb blockade effect. The drastic increase in $|MR|$ is observed as temperature decreased from 25 to 4.2 K. This feature is more distinct than that in conventional FM-I granular systems, which can be ascribed to the prominent cotunneling effect in the Coulomb blockade regime due to the size uniformity of the monodispersed cluster assemblies employed in this study.

ACKNOWLEDGMENTS

This work has been supported by Core Research for Evolutional Science and Technology (CREST) of the Japan Science and Technology Corporation (JST), and partly by a Grant-in-Aid for Scientific Research A1 (Grant No. 08505004). We appreciate Dr. M. Sakurai for his useful comment and thank Dr. Takahashi and Professor Maekawa for helpful discussions. We are also indebted to the support from the Laboratory for Development Research of Advanced Materials of IMR.

[1] W. H. Meiklejohn and C. P. Bean, Phys. Rev. **102**, 1413 (1956); **105**, 904 (1957).
[2] S. Gangopadhyay, G. C. Hadjipanayis, B. Dale, C. M. Sorensen, K. J. Klabunde, V. Papaefthymiou, and A. Kostikas, Phys. Rev. B **45**, 9778 (1992).
[3] F. J. Darnell, J. Appl. Phys. **32**, 186S (1961).
[4] S. Gangopadhyay, G. C. Hadjipanayis, C. M. Sorensen, and K. J. Klabunde, IEEE Trans. Magn. **28**, 3174 (1992).
[5] S. Gangopadhyay, G. C. Hadjipanayis, C. M. Sorensen, and K. J. Klabunde, J. Appl. Phys. **73**, 6964 (1993).
[6] T. Uchikoshi, Y. Sakka, M. Yoshitake, and K. Yoshihara, Nanostruct. Mater. **4**, 199 (1994).
[7] Y. D. Yao, Y. Y. Chen, C. M. Hsu, H. M. Lin, C. Y. Tung, M. F. Tai, D. H. Wang, K. T. Wu, and C. T. Suo, Nanostruct. Mater. **6**, 933 (1995).
[8] D. L. Peng, K. Sumiyama, S. Yamamuro, T. Hihara, and T. J. Konno, Appl. Phys. Lett. **74**, 76 (1999).
[9] Jagadeesh S. Moodera, and Lisa R. Kinder, J. Appl. Phys. **79**, 4724 (1996).
[10] M. Julliere, Phys. Lett. **54A**, 225 (1975).
[11] S. Maekawa and Gäfvert, IEEE Trans. Magn. **18**, 707 (1982).
[12] J. C. Slonczewski, Phys. Rev. B **39**, 6995 (1989).
[13] J. S. Moodera, L. R. Kinder, T. M. Wong, and R. Meservey, Phys. Rev. Lett. **74**, 3273 (1995).
[14] T. Miyazaki and N. Tezuka, J. Magn. Magn. Mater. **139**, L231 (1995).
[15] J. S. Helman and B. Abeles, Phys. Rev. Lett. **37**, 1429 (1976).
[16] H. Fujimori, S. Mitani, and S. Ohnuma, Mater. Sci. Eng., B **31**, 219 (1995).
[17] P. Sheng, B. Abeles, and Y. Arie, Phys. Rev. Lett. **31**, 44 (1973).
[18] M. Roilos and P. Nagels, Solid State Commun. **2**, 285 (1964).
[19] S. Yamamuro, K. Sumiyama, M. Sakurai, and K. Suzuki, Supramol. Sci. **5**, 239 (1998); J. Appl. Phys. **85**, 483 (1999).
[20] S. Yamamuro, K. Sumiyama, T. Hihara, and K. Suzuki, J. Phys.: Condens. Matter. **11**, 3247 (1999).
[21] C. C. Tsuei and R. Hasegawa, Solid State Commun. **7**, 1581 (1969).
[22] R. W. Cochrane, R. Harris, J. O. Ström-Olson, and M. J. Zuckermann, Phys. Rev. Lett. **35**, 676 (1975).
[23] H. Sato, I. Sakamoto, and C. Fierz, J. Phys.: Condens. Matter **3**, 9067 (1991).
[24] C. Uher, R. Clarke, G. Zheng, and I. K. Schuller, Phys. Rev. B **30**, 453 (1984).
[25] M. T. Perez and J. L. Vicent, Phys. Rev. B **38**, 9503 (1988).
[26] H. Fujimori, S. Mitani, S. Ohnuma, T. Ikeda, T. Shima, and T. Masumoto, Mater. Sci. Eng., A **181/182**, 897 (1994).
[27] A. Carl, G. Dumpich, and D. Hallfarth, Phys. Rev. B **39**, 915 (1989); **39**, 3015 (1989); Thin Solid Films **193/194**, 1065 (1990).
[28] B. L. Altshuler, A. G. Aronov, and P. A. Lee, Phys. Rev. Lett. **44**, 1288 (1980).
[29] G. Deutscher, B. Bandyopadhyay, T. Chui, P. Lindenfeld, W. L. McLean, and T. Worthington, Phys. Rev. Lett. **44**, 1150 (1980).
[30] D. Stauffer, Phys. Rep. **54**, 1 (1979).
[31] C. A. Neugebauer and M. B. Webb, J. Appl. Phys. **33**, 74 (1962).
[32] B. Abeles, Ping Sheng, M. D. Coutts, and Y. Arie, Adv. Phys. **24**, 407 (1975).
[33] K. Ono, H. Shimada, S. Kobayashi, and Y. Ootuka, J. Phys. Soc. Jpn. **65**, 3449 (1996).
[34] K. Ono, H. Shimada, and Y. Ootuka, J. Phys. Soc. Jpn. **66**, 1261 (1997).
[35] L. F. Schelp, A. Fert, F. Fettar, P. Holody, S. F. Lee, J. L. Maurice, F. Petroff, and A. Vaures, Phys. Rev. B **56**, R5747 (1997).
[36] S. Mitani, S. Takahashi, K. Takanashi, K. Yakushiji, S. Maekawa, and H. Fujimori, Phys. Rev. Lett. **81**, 2799 (1998).
[37] S. Takahashi and S. Maekawa, Phys. Rev. Lett. **80**, 1758 (1998).